



Québec, QC
10 au 13 juin 2008 / June 10-13, 2008

PERFORMANCE OF AUTOMATED PROJECT PROGRESS TRACKING WITH 3D DATA FUSION

F. Bosche¹, C. T. Haas², P. Murray³

¹ PhD Candidate, Department of Civil Engineering, University of Waterloo, Waterloo, Ontario, Canada.

² Professor and Tier I Canada Research Chair, Department of Civil Engineering, University of Waterloo, Waterloo, Ontario, Canada.

³ Site Manager, SNC-Lavalin, Power Ontario Inc.

Abstract: In the Architectural-Engineering-Construction & Facility Management industry, project progress tracking is an important management task. Currently, this task still requires a significant amount of non value-adding manual effort that interferes with value-adding work. Additionally, current practice may lead to approximate or unreliable results. In this paper, the authors present an approach fusing three-dimensional (3D) Computer-Aided Design (CAD) modeling and time-stamped 3D laser scanned data for non intrusive automated project progress tracking. This approach robustly and efficiently recognizes all 3D CAD model elements in project 3D laser scans. Its applicability and performance with respect to automated construction progress tracking are investigated. Real-life data obtained during the construction of a green field power plant project is used for the investigation.

1. Background

The Architectural-Engineering-Construction & Facility Management (AEC&FM) industry needs to conduct many performance control activities that require the assessment of the life-cycle three-dimensional (3D) status of projects. Such activities include construction progress and productivity tracking and dimensional quality assessment and quality control (QA/QC). The authors note that, currently, these activities are performed using means that are labour-demanding and provide incomplete and sometimes erroneous results. For instance, construction progress is often controlled by using foremen daily reports to estimate the current progress and comparing this estimated progress against the scheduled progress; and dimensional QA/QC is performed using tools such as measurement tapes, levels, total stations and by comparing the measurements against written specified dimensions. The focus of this paper is on construction progress control.

Research has been and is being conducted in investigating the use of new technologies for more efficient, reliable and automated construction progress control. These research efforts have focused on: Construction progress visualization tools (Poku and Arditi 2006); as well as Progress information collection systems using digital pictures (Abeit and Arditi 2003; Brilakis and Soibelman 2005), Global Navigation Satellite Systems (GNSSs) (Caldas et al. 2006; Navon 2007), barcodes (Chen et al. 2005; Echeverry 1996; Navon 2007) and/or RFID tags (Ergen et al. 2006; Razavi et al. 2008). The approach developed by the authors and presented here can be used as an alternative or complementary approach to the latter ones for acquiring site 3D information. It especially enables the automated tracking of project 3D information. It is expected to be very robust and fully automated.

The use of 3D Computer-Aided Design (CAD) modeling is spreading in the AEC&FM industry. With respect to 3D project status assessment, it can be noted that a project 3D CAD model is a representation of the project 3D specifications that is «3D-organized». Then, laser scanning (also referred to as LADAR scanning) is being introduced to the industry as an efficient and robust means to acquire comprehensive and high quality site 3D status information that is also 3D-organized. By taking advantage of this correspondence, 3D laser scans and 3D CAD models could be compared – more exactly, 3D model information could be recognized in the 3D laser scans – enabling as-built 3D status tracking.

The authors have developed a novel approach for automated recognition of project 3D CAD model objects in site 3D laser scans. The approach is summarized in Section 2. A more complete description (although it is still being improved) can be found in (Bosche and Haas 2008). Section 3 describes how this approach can be used to perform automated 3D progress tracking. Section 4 presents an experiment conducted with real-life data to investigate the feasibility and performance of this application.

2. The 3D Data Fusion Approach

The developed approach considers the entire 3D CAD model of a project in order to recognize all the 3D objects that constitute it, so that occlusions of CAD objects due to other CAD objects, referred to as *internal occlusions*, are taken into account, which increases the performance of the approach. This approach consists of a series of five consecutive steps:

- 1 *Convert the 3D CAD model.* In order to use the 3D information contained in the 3D CAD model, full access to the model description is required, in particular the 3D description. 3D CAD models are generally stored in protected proprietary 3D CAD engine formats (e.g. DXF, DWG, DGN, etc.). An adequate open-source format thus had to be identified for this research. Many open-source CAD formats exist such as the Industry Foundation Classes (IFC). Here, the STereoLithography (STL) format is chosen. The STL format is a 3D data representation based on triangular facet approximation. It is chosen because it not only allows the conversion of the 3D model without the loss of too much 3D information, but it also enables a significant simplification of the step 3 of this approach.
- 2 *Register both data sets.* Scanner and 3D model registration information is used to reference the STL-formatted project 3D model in the scanner's spherical coordinate frame.
- 3 *Calculate the as-planned scan.* For each as-built scanned range point, a corresponding as-planned range point is calculated. It is first assigned the same pan and tilt angles as the ones of the as-built point. Its range is then calculated by performing the virtual single point scan defined by this direction and the 3D CAD model as the virtually scanned world. If the scanning direction intersects an object STL facet, the range is calculated as the distance between the scanner and the intersection point. The as-planned point is additionally assigned as an *IDobject* feature, the name or ID of the object to which the intersected facet belongs. A point that does not intersect any STL facet is assigned an infinite range and a null *IDobject* value.

A rapid analysis of this process may lead to the conclusion that the calculation of each as-planned point requires investigating the intersection of its scanning direction with each object, or more exactly each object STL facet, and consequently that its complexity is linearly proportional to the product of the number of model STL facets and the number of scanned points, which can be significant. However, it can be shown that a scanning direction can only intersect a facet whose bounding pan and tilt angles surround the scanning direction angles, so that the calculation of all the as-planned point ranges can be performed with a complexity independent from the number of model STL facets (and thus of the number of model objects). This complexity reduction is enabled by the use of the STL format. This format in fact not only enables reducing the amount of calculations to be done, but it also enables a simpler calculation of each as-planned point range. Indeed, with this format, the calculation of each as-planned point range simply requires the calculation of the intersections of a line (the point scanning direction) with

triangles (STL facet). If other 3D formats based on primitive forms were used, the calculation of each as-planned point range would require the calculation of the intersections of the point scanning direction with primitive forms (or combinations of primitive forms), which is far more complex.

- 4 *Recognize the as-planned points.* Once this as-planned scan is completed, the as-planned points can be sorted by their *IDobject* feature, so that each object is assigned an as-planned range point cloud. Then, for each object, each as-planned point can be matched to its corresponding as-built point. This requires a *point recognition metric*. Since the two corresponding points share the same pan and tilt angles, only their ranges need to be compared. The chosen point recognition metric is the comparison of the difference between the as-built and as-planned point ranges, $\Delta\rho$, with a pre-defined threshold, $\Delta\rho_{\min}$. If the absolute value of $\Delta\rho$ is smaller than $\Delta\rho_{\min}$, then the point is recognized; it is not otherwise.

The estimation of $\Delta\rho_{\min}$ could be automatically customized for each point by considering many scanning parameters including: the point as-planned pan angle, tilt angle and range, reflection angle (angle between the scanning direction and the scanned surface normal vector) and reflectivity (the reflectivity of the surface from which the as-planned point is obtained); the scanner pan and tilt angle measurement uncertainties; and the model-scan registration error. However, this would require the estimation of the relations between $\Delta\rho_{\min}$ and all these parameters *a priori*. For this, multiple experiments with complex setups would need to be conducted, which is out of the scope of this research.

A simpler, but still robust, $\Delta\rho_{\min}$ threshold estimation is used in the research. One of the above characteristics is retained: for each scan, $\Delta\rho_{\min}$ is set so that it is greater than the mean registration error, ϵ_{Reg} (Equation 1). ϵ_{Reg} is the mean distance between the tie points in the model and in the scan once the model-scan registration has been performed, so that it provides a general idea of the expected alignment between the scan and the model. The formula in Equation 1 also takes into account possible construction location errors by adding 50 mm to ϵ_{Reg} .

$$[1] \Delta\rho_{\min} = \epsilon_{\text{Reg}} + 50 \text{ mm}$$

5. *Recognize the objects.* For each object, once all its as-planned cloud points have been matched to their corresponding as-built points, it can be inferred whether the object is itself recognized or not. This requires an *object recognition metric*. The chosen metric is based on the object recognized surface. For each object, the recognized surface, Surf_R , is calculated as the weighted sum of its recognized points, where each point weight is its *as-planned covered surface*. The covered surface of an as-planned point is roughly defined as the area delimited by the equidistant boundaries between it and its immediate neighboring points. It is calculated as a function of the scan angular resolution, the as-planned point range and the as-planned point reflection angle – the angle between the point scanning direction and the normal to the STL facet from which it is obtained (see (Bosche et al. 2008) for more details). Then, the object recognition metric compares Surf_R to a threshold Surf_{\min} . If Surf_R is larger Surf_{\min} , then the object is recognized; it is not otherwise.

The value of Surf_{\min} is automatically estimated using the formula presented in Equation 2. This formula takes into account the scan angular resolution (Res_ϕ and Res_θ) and the maximum distance between the scanner and the model ($\text{Model}.\rho_{\max}$), so that this object recognition metric is invariant with the scan angular resolution and the scanner-object distance. The calculation of Surf_{\min} also requires a value for n be chosen *a priori*. n is the minimum number of points to be recognized at a distance $\text{Model}.\rho_{\max}$ so that their total covered surface equals Surf_{\min} . This ensures that no object can be recognized if less than n of its as-planned points are recognized. The authors chose for their experiments a value of $n=5$ points. This value should result in a good compromise between a high recall, precision and specificity performance rates.

$$[2] \text{Surf}_{\min} = n \cdot \tan(\text{Res}_\phi) \cdot \tan(\text{Res}_\theta) \cdot (\text{Model}.\rho_{\max})^2$$

In (Bosche et al. 2008), the authors demonstrate that these methods for the automated estimations of $\Delta\rho_{\min}$ and Surf_{\min} (Equations 1 and 2) are very efficient and lead to high recognition performances. Additionally, this approach enables the recognition of partially built or occluded objects, so that it is suited to recognize not only full non-occluded objects (e.g. non-occluded built-in-place or pre-fabricated elements), but also objects being highly occluded as well as objects being progressively built in place, (e.g. brick walls), which are very common cases in site laser scans.

3. Automated 3D Progress Tracking Strategy and Performance Assessment

The developed approach enables the efficient and automated recognition of 3D CAD model objects in site laser scans. As a result, if laser scans are obtained from a given site at different construction stages, it is theoretically possible to automatically infer, from the recognition results obtained with them, the construction progress between two stages.

As an example, consider a project with its 3D model. Scans may be conducted at different days but also in a same day from different locations and in different directions. Consider $\{S\}_{d_1}$ and $\{S\}_{d_2}$, the sets of scans conducted at respectively day d_1 and d_2 , where d_1 precedes d_2 . The developed approach can be used to recognize the 3D model objects in each scan of $\{S\}_{d_1}$ and $\{S\}_{d_2}$, and construction progress between the days d_1 and d_2 can then be inferred by identifying the objects that are recognized in $\{S\}_{d_2}$ but not in $\{S\}_{d_1}$. Note that this is only an estimation of the true progress. In fact, three *levels* of progress must be distinguished:

The *true progress* of the project,

The *scanned progress*, which is the portion of the true progress that is captured with $\{S\}_{d_1}$ and $\{S\}_{d_2}$, and

The *recognized progress* which is the portion of the scanned progress that is inferred from the object recognition results obtained using the developed approach with $\{S\}_{d_1}$ and $\{S\}_{d_2}$.

There are therefore two sources of errors that may impact the performances of a progress tracking system based on the developed approach: (1) the incomplete capture of the progress with the different scans, and (2) the limited object recognition performances of the developed approach. Section 4 presents an experiment, using real-life data, investigating the feasibility and performance of using the developed approach for automated construction 3D progress tracking.

4. Experiment

In this experiment, data obtained from the construction of a building that is part of a power plant project in downtown Toronto is used (see acknowledgements in Section 6). The building is 60m long by 15m wide by 9.5m high. It has a steel structure, the construction of which was the focus of the conducted experiments. Figure 1 presents a picture, the 3D CAD model, and one scan of the building steel structure. The complete 3D model, once STL-formatted, contains 612 objects with a total of 19,478 facets. The laser scanned data used in the experiments was obtained with a Trimble™ GX 3D scanner that uses time-of-flight technology. The scanned data consists of five scans conducted from different locations and on two different days about one week apart. The days are referred to as d_1 and d_2 , where d_1 precedes d_2 . Two scans were obtained at d_1 and three at d_2 . Information about these scans is provided in Table 1.

The experiment described here includes two parts. First, the performance of the developed approach for the recognition of the 3D model objects in the five scans is analyzed. Then, the results are used to investigate its resulting performance for recognizing project 3D progress. In these two experiments, recognition performance is evaluated using recall, specificity and precision rates. It must be noted that the calculation of these performance measures required the manual estimation of which objects are

actually present in each scan as well as which objects are actually part of the progress between d_0 and d_1 , and d_1 and d_2 , where d_0 is the day zero of construction when no project element is yet built or installed. This manual estimation, the results of which are presented in Table 1, might have resulted in some errors. Nonetheless, it has been performed conservatively — if there is a doubt on the presence of an object, this one is considered present — so that the results can only be biased toward lower performances.

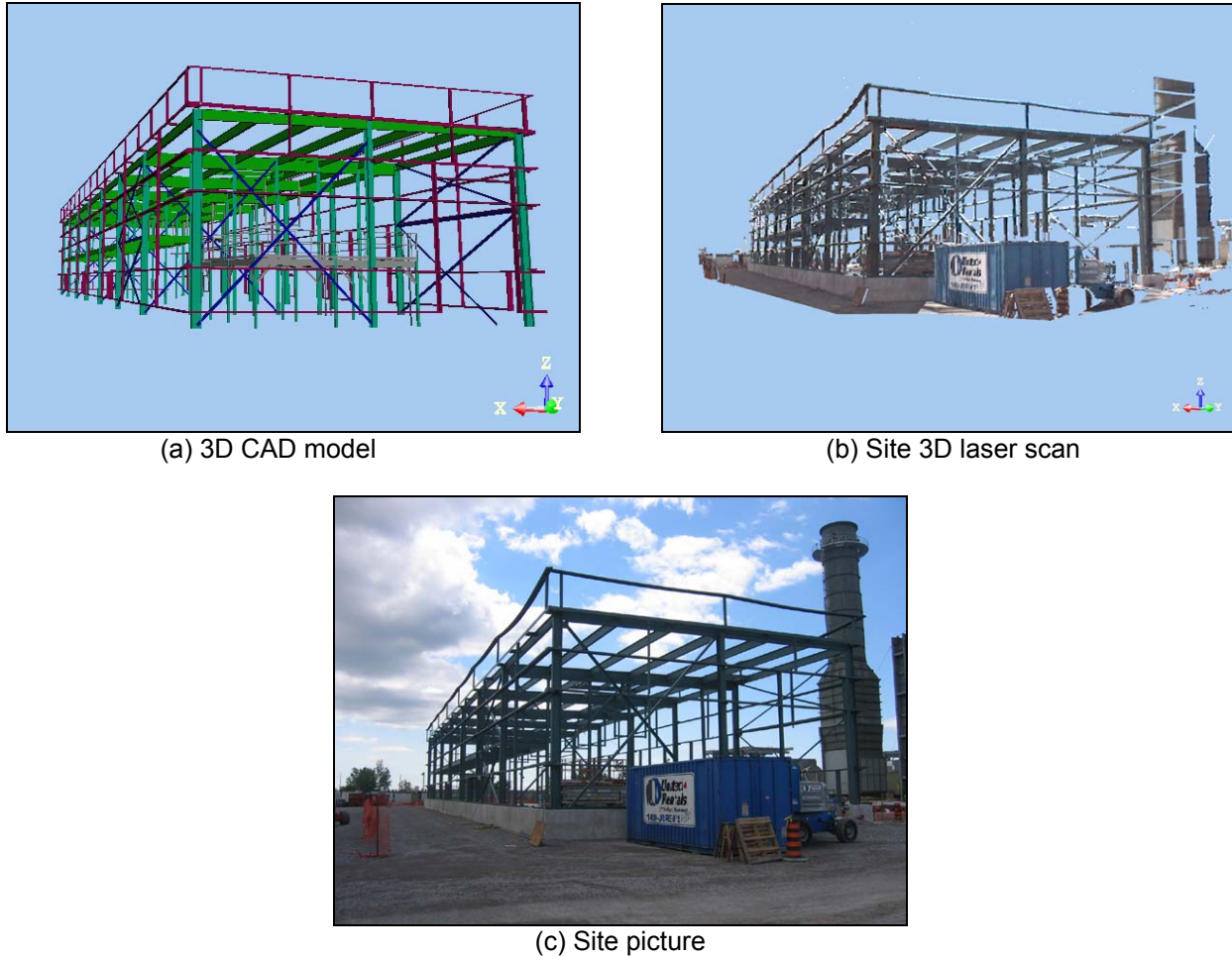


Figure 1: the 3D Model, one site 3D laser scan and a site picture of the investigated PEC building.

Table 1: Scans identification and characteristics

Scan day	Scan Number	Number of points	Angular resolution	Number of search CAD objects observable in scan
d_1	1	691,906	Pan: 582 μ rad Tilt: 582 μ rad	321
d_1	2	723,523	Pan: 582 μ rad Tilt: 582 μ rad	286
d_2	1	810,399	Pan: 582 μ rad Tilt: 582 μ rad	302
d_2	2	650,941	Pan: 582 μ rad Tilt: 582 μ rad	271
d_2	3	134,263	Pan: 300 μ rad Tilt: 300 μ rad	38

4.1 Object Recognition

Figure 2 displays, as an example, the object recognition results obtained with the scan 2 of day d_2 . Table 2 summarizes the results and performances obtained with the five scans. In this table, object recognition performance is measured using recall, specification and precision rates. For a given scan, these performance measures are defined as:

Recall rate: the number of search objects that are recognized and truly are in the scan divided by the total number of search objects that truly are in the scan.

Specificity rate: the number of search objects that are not recognized and are truly not in the scan divided by the total number of search objects that are truly not in the scan.

Precision rate: the number of search objects that are recognized and truly are in the scan divided by the total number of search objects that are recognized in the scan.

It appears in Table 2 that the approach achieves very high specificity and precision rates in all cases. The underlying performance is that it is very robust not to recognize an object that is not in a scan. Then, the approach achieves slightly lower, but still good, recall rates. A more detailed analysis of the results actually shows that low recall rates are particularly obtained with small objects (e.g. wall panel braces), while high recall rates are obtained with larger objects (e.g. column, beam). These small objects are also the reason for the false positive recognitions. Indeed, a small object next to a big object can be easily mis-recognized, especially if significant 3D registration errors are observed (see discussion below). It must be noted that, in the investigated problem of 3D progress control, the mis-recognition of small objects is not necessarily a critical issue, since these would often not significantly impact the overall progress estimation.

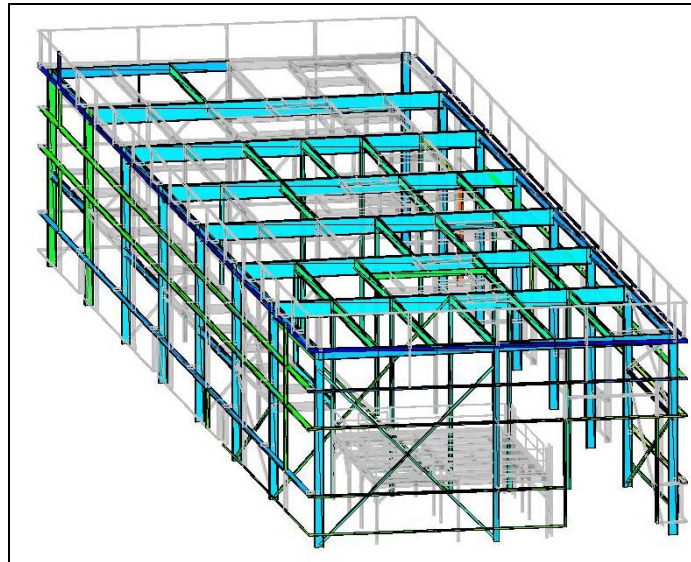


Figure 2: Example with the scan 2 from day d_2 of object recognition results (the recognized objects are colored and are opaque. Those that are not recognized are light grey and transparent).

Another significant source of error for this approach, and particularly in this set of experiments, is 3D model-scan registration. Indeed, the mean registration error observed for the five scans is in average equal to 30 mm. While the estimation of $\Delta\rho_{\min}$ partially takes this error into account, this error remains significant and has a considerable impact on the object recognition results. Note that the reason for these high mean registration error values is that registration was performed by manual point matching was

used. In the industry, scan registration error specifications are far more stringent with values of a couple of millimetres. For achieving such accuracies, precisely located project *tie points* are used. With mean registration errors of a couple of millimetres, it is expected that the recognition results presented here would have resulted in far better performances.

Finally, It can be noted in the results presented in Table 2 that combining the object recognition results of different scans from a same day increases, sometimes significantly, the overall recall rate without considerably impacting the specificity and precision performances.

Table 2: Object recognition results for the different scans of day d_1 (values are numbers of objects).

Scan Day – N°	Objects Automatically Recognized	Objects Scanned (manually observed in scan)		Recall	Specificity	Precision
		No	Yes			
$d_1 - 1$	No	266	76	79%	92%	91%
	Yes	24	255			
$d_1 - 2$	No	301	72	75%	93%	90%
	Yes	23	216			
$d_1 - \text{Combined}$	No	200	64	83%	86%	91%
	Yes	33	315			
$d_2 - 1$	No	284	81	73%	92%	89%
	Yes	26	221			
$d_2 - 2$	No	321	60	78%	94%	92%
	Yes	19	212			
$d_2 - 3$	No	568	9	76%	99%	83%
	Yes	6	29			
$d_2 - \text{Combined}$	No	216	60	84%	88%	91%
	Yes	30	306			

4.2 Progress Recognition

The second stage of this experiment is to assess the feasibility and performance of using the results obtained with the developed approach to recognize progress. Table 3 summarizes the progress recognition results and performances using the results obtained with the developed approach for the periods d_0-d_1 , and d_1-d_2 . In this experiment, the *scanned progress* and *recognized progress*, defined earlier, are estimated, for a period d_i-d_{i+1} , as:

Scanned progress: An object is considered part of the scanned progress if it is not found by manual observation in any scan of day d_i and is manually observed in at least one scan of day d_{i+1} .

Recognized progress: An object is considered part of the automatically recognized progress if it is automatically recognized in any scan of day d_{i+1} and is not found by manual observation in any scan of day d_i .

It is acknowledged that the latter definition should be “an object is considered part of the automatically recognized progress if it is automatically recognized in any scan of day d_{i+1} and is not automatically recognized in any scan of day d_i ”. However, in order to properly assess the performance of inferring progress using the object recognition results obtained with the developed approach, it is important that the status of the project at the beginning of each investigated period, at d_i , be known accurately. While the object recognition results of d_i should be used in practice for that purpose, the object recognition results obtained with the data sets used here are not sufficiently good – for the reasons discussed in Section 4.1. As a result, visually identified objects of d_i are used as the estimation of the project 3D status at d_i .

Then, the recall, specification and precision rates calculated in Table 3 are defined as:

Recall rate: the number of search objects that are recognized as part of the scanned progress (recognized progress) and truly are in scanned progress divided by the total number of search objects that truly are in the scanned progress.

Specificity rate: the number of search objects that are not recognized as part of the scanned progress and are truly not in the scanned progress divided by the total number of search objects that are truly not in the scanned progress.

Precision rate: the number of search objects that are recognized as part of the scanned progress and truly are in the scanned progress divided by the total number of search objects that are recognized as part of the scanned progress.

Table 3: Progress recognition results for the period d_0 to d_1 (values are numbers of objects).

Period°	Objects Automatically Recognized As Part of the Progress	Objects Scanned As Part of the Progress (manually observed in scans)		Recall	Specificity	Precision
		No	Yes			
$d_0 - d_1$	No	200	64	83%	86%	91%
	Yes	33	315			
$d_1 - d_2$	No	576	2	78%	96%	21%
	Yes	27	7			

The results in Table 3 show that progress is quite successfully automatically recognized (high recall rates). For the period d_0-d_1 , the results are actually those obtained for the object recognition in the scans of $\{S\}_{d_1}$ (see Table 2). They are good, but cannot be used to arguably conclude with respect to the performance of the proposed approach for automated construction progress. The results obtained for the period d_1-d_2 are more meaningful in that regard. First, it appears that most of the scanned progress over that period is automatically recognized (high recall rate). Only two of the visually identified nine objects are not recognized. These two objects are actually both visually identified in Scan 3 but not recognized in that scan. Further analysis shows that these two objects are small. Additionally, their recognized surface in Scan 3 is 0.002 m^2 and 0.008 m^2 . The fact that these are not null means that some of their as-planned range points are in fact recognized in the scan, but their covered surfaces are smaller than Surf_{\min} that equals 0.011 m^2 . So, not only these two objects are almost recognized, but they are both small, so that the fact that they are not recognized has a small impact on the overall progress recognition performance.

Then, most of the scanned *non-progress* (objects not part of the progress) is also automatically recognized (high specificity rate). However, 27 objects are recognized as part of the progress during the period d_1-d_2 although they are truly not. This means that they are recognized in at least one of the scans of $\{S\}_{d_2}$, and are not visually identified in any scan of $\{S\}_{d_1}$. This is actually to be related to the object recognition results obtained with the scans of d_2 . Indeed, as can be seen in Table 2, 30 objects are recognized in at least one scan of $\{S\}_{d_2}$ although they are not in any of these scans. The reasons for these Type II errors have been identified in Section 4.2:

The small sizes of these objects, which implies that they are generally not critical in terms of progress tracking.

The poor 3D registration quality, which has more impact on smaller objects.

So, overall, it can be concluded that, considering the lower quality of the data sets used in these experiments, the 3D progress recognition results obtained are fairly good and prove the feasibility of using the developed approach for tracking construction 3D progress.

However, as discussed earlier, this feasibility analysis uses manually observed information about which objects are in the scans at day d_i in order to evaluate the accuracy of the estimate of the progress at day d_{i+1} . In order to fully automate 3D progress tracking in practice, another method must be used. The authors propose to take advantage of 4D models instead of 3D models. A project 4D model is the result of the fusion of its 3D model and its CPM schedule. Using a 4D CAD model and the physically derived precedence relationships from the CPM schedule, the 4D model at day d_i can be used to provide a good estimate of the objects that are already built at that day.

This approach is beneficial only if the CPM schedule is sufficiently detailed and well updated. From current practice, it is however clear that most projects proceed only in the most general form with respect to their schedules and most individual activities are generally offset by days and weeks from their original schedule dates. But, it must be noted that, if the proposed approach using the 4D model is used from day d_0 , then this problem can be overcome. Indeed, since the progress at d_0 is well known – nothing is yet built, the developed approach can achieve good object and progress recognition results at day d_1 . These results can be used to update the CPM schedule (and consequently the 4D model) at d_1 , enabling better automated 3D progress recognition results at day d_2 . This procedure is then reiterated at day d_2 and until the end of the project, enabling good 3D progress recognition performances during the entire length of the project.

Note, one other source of *a priori* information may be used from the 4D model, further increasing the object and progress recognition results. For each 3D laser scan acquired at a day d_i , the corresponding virtual scan used for the object recognition can be calculated using the 4D model at day d_i . The virtual scan obtained this way would more likely match the real scan, in particular with regard to model internal occlusions.

Finally, the physically derived precedence relationships from the CPM schedule can also be used to recognize with reasonable confidence objects which are not recalled in day's fused scans and yet can be inferred to exist due to the recognition of successor elements.

4.3 Scanned Progress vs. True Progress

It must be noted that only the scanned progress can be recognized. Therefore, if the scanned progress significantly differs from the true progress, the recognized progress will be misleading. It is thus important to ensure that the scanned progress actually reflects the true progress. This can be done by conducting many scans from many locations and in many directions. However, this would also require the processing of many scans, with often redundant results.

The developed approach actually enables a better solution to this problem. Indeed, it builds a virtual scan to be compared to the actual scan. Therefore, before the construction of a project is even started, scanners could be virtually positioned and scans virtually conducted. The results of these virtual scans could be used to optimize the number and positions of scans to effectively capture relevant project 3D status information for tracking the project 3D progress during its entire construction. In other words, the developed approach enables *planning for scanning*.

Finally, another means to improve the overall tracking of project 3D status is data fusion. Fusing with the laser scanned data, field data obtained with other technologies, such as Radio Frequency and IDentification (RFID) tags – these are already used to track prefabricated elements, would help improve the quality and quantity of collected field information and thus improve the overall performance of object and progress recognition.

5. Conclusion

In this paper, the authors investigate the feasibility and performance of using a new approach for automated project 3D CAD model object recognition in construction site laser scans for conducting automated construction 3D progress tracking. First, the recognition approach performs well for automatically recognizing 3D model objects in laser scans. Then, it has been shown that it can provide sufficiently good results to enable automated construction 3D progress tracking. Since the developed object recognition approach can robustly recognize 3D model objects that are partially built or occluded, it enables the tracking of the progress of the construction of not only pre-fabricated and installed project elements, but also elements that are progressively built in place.

6. Acknowledgement

This project is funded by the Canada Research Chair in Construction & Management of Sustainable Infrastructure. The authors would also like to thank the company SNC-Lavalin for its support for this research, in particular for allowing Frederic Bosche come in its PEC project site, conduct some scanning, as well as publish these results.

7. References

- Abeit, J., and Arditi, D. (2003). "Photo-Net: An Integrated System for Controlling Construction Progress." *Journal of Engineering, Construction and Architecture Management*, 10(3), 162-171.
- Bosche, F., and Haas, C. T. (2008). "Automated Retrieval of 3D CAD Model Objects in Construction Range Images." *Journal of Automation in Construction*, 17(4), 499-512.
- Bosche, F., Haas, C. T., and Akinci, B. (2008). "Performance of a New Approach for Automated 3D Project Performance Tracking." *ASCE Journal of Computing in Civil Engineering, Special Issue on 3D Visualization*, Submitted.
- Brilakis, I. K., and Soibelman, L. "Identification of Materials from Construction Site Images Using Content Based Image Retrieval Techniques." *ASCE International Conference on Computing in Civil Engineering*, Cancun, Mexico.
- Caldas, C., Grau, D., and Haas, C. (2006). "Using Global Positioning Systems to Improve Materials Locating Processes on Industrial Projects." *Journal of Construction Engineering and Management*, 132(7), 741-749.
- Chen, S.-C., Shyu, M.-L., Peeta, S., and Zhang, C. (2005). "Spatiotemporal vehicle tracking: the use of unsupervised learning-based segmentation and object tracking." *IEEE Robotics and Automation Magazine*, 12(1), 50-58.
- Echeverry, D. "Adaptation of Barcode Technology for Construction Progress Control." *ASCE Journal of Computing in Civil Engineering*, New-York, USA, 1034-1040.
- Ergen, E., Akinci, B., and Sacks, R. (2006). "Tracking and Locating Components in a Precast Storage Yard Utilizing Radio Frequency Identification Technology and GPS." *Automation in Construction*, 16(2), 354-367.
- Navon, R. (2007). "Research in Automated Measurement of Project Performance Indicators." *Automation in Construction*, 16(2), 176-188.
- Poku, S. E., and Arditi, D. (2006). "Construction Scheduling and Progress Control using Geographical Information Systems." *ASCE Journal of Computing in Civil Engineering*, 20(5), 351-360.
- Razavi, S. N., Young, D., Nasir, H., Haas, C., Caldas, C., and Goodrum, P. "Field Trial of Automated Material Tracking in Construction." *CSCCE 2008 conference*, Québec, QC, Canada.